Methodology for the simulation of a ship's damage stability and ultimate strength conditions following a collision

Citation for the original published paper (version of record):
Kuznecovs, A., Schreuder, M., Ringsberg, J. (2021). Methodology for the simulation of a ship's damage stability and ultimate strength conditions following a collision. Marine Structures, 79(1): 1-19.
http://dx.doi.org/10.1016/j.marstruc.2021.103027

Marine Structures 79 (2021) 103027

Contents lists available at ScienceDirect

Marine Structures

journal homepage: www.elsevier.com/locate/marstruc

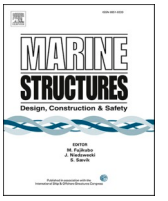

Methodology for the simulation of a ship's damage stability and ultimate strength conditions following a collision

Artjoms Kuznecovs, Martin Schreuder, Jonas W. Ringsberg *

Chalmers University of Technology, Department of Mechanics and Maritime Sciences, Gothenburg, Sweden

ARTICLE INFO

Keywords:
Accidental limit state
Damage stability
Progressive collapse
Progressive flooding
Safety
Ship collision
Ultimate limit state

ABSTRACT

This paper presents a methodology called SHARC developed for the simulation and analysis of a ship's damage stability and ULS conditions following a collision. SHARC combines three types of methods: advanced nonlinear finite element simulations that simulate the collision scenario, a dynamic damage stability simulation tool called SIMCAP, and a modified Smith method for the ULS analysis of a collision-damaged ship structure. The novelty of the presented methodology is that it can be used for real-time simulations to study the ingress of water through the damage opening of a struck vessel and how it affects the ship's stability, structural integrity (ULS) and survival capability against, e.g., capsizing. The results for an intact and a damaged oil tanker under noncorroded and corroded structural conditions and various sea states are presented to demonstrate the features of SHARC.

1. Introduction

Ship collisions can lead to serious consequences. The accidental limit state (ALS) approach can be used in the design of ship structures to analyze hazardous consequences that could be avoided/mitigated beforehand in the design stage of a structure [1]. The ALS design in this context has three main objectives: (i) to avoid loss of life in those structures involved in a collision event or the surrounding area, (ii) to avoid polluting the environment, and (iii) to minimize loss of property or financial exposure.

In the ship-collision ALS design, a ship design should be achieved such that the main safety functions of the structure are not impaired during an accidental event or within a certain time period after an accident. Since the structural damage characteristics and the behavior of damage structures depend on the type of accident, the establishment of universally applicable structural design criteria for the ALS is not straightforward. Numerous possible scenarios can be relevant for the analysis of collision events. Thus, for a given type of structure, design accidental scenarios and associated performance criteria must be chosen on the basis of a risk assessment. Once a set of accidental scenarios that can represent critical events has been identified, refined computations can be performed for advanced safety studies. Paik [1] proposed that a set of realistic collision scenarios (with a limited number) can be obtained by making use of probabilistic sampling techniques according to the following procedure: (i) choose the collision event, (ii) identify the hazard, (iii) identify random parameters affecting the event, (iv) identify data sources, (v) choose the probabilistic density functions, and (vi) use sampling techniques that lead to the selection of event scenarios for refined computations.

* Corresponding author.
E-mail address: Jonas.Ringsberg@chalmers.se (J.W. Ringsberg).

https://doi.org/10.1016/j.marstruc.2021.103027
Received 15 January 2021; Received in revised form 24 March 2021; Accepted 15 May 2021
Available online 24 May 2021

1.1. Damage stability of ships

For a ship that receives hull damage from a collision, its damage stability conditions will change due to flooding or the outflow of cargo from its compartments and cargo holds. The survivability of a ship is often seen as the survivability of people onboard the ship, where the time available to evacuate and abandon the ship, which can be estimated by time-domain predictions of progressive flooding, is crucial. Santos and Guedes Soares [2] presented a mathematical model in the time domain of the motions and flooding of ships in a seaway that was applied in simulations of the behavior of a damaged Ro-Ro ship. Parametric studies were carried out to investigate how, e.g., transient flooding, the flow rate in various compartments and the effect of floodwater on the roll motion affected the evacuation and capsizing times.

Bennet and Phillips [3] presented an experimental investigation into the influence of floodwater and transient flooding on the motions and structural response of a ship hull following a grounding incident. Their results showed that floodwater had a significant effect on the magnitude of ship responses. The movement of the floodwater free surface showed some substantial second-order sloshing effects close to the ship peak response but little movement in higher-frequency waves. They concluded that in comparison with classification design rules, further assessment of the safety margins, including an investigation of global responses in conjunction with any local loading due to the presence of floodwater, is needed. Ruponen et al. [4] presented an approach for analyzing the level of survivability for a collision-damaged passenger ship. Monte Carlo simulations were used to generate a large number of damage cases, each of which was calculated with a time-domain flooding simulation. The survivability of the ship was analyzed based on requirements for sufficient reserve stability. Various ship design changes were studied for comparison purposes to propose safer ship designs.

In the review paper by Manderbacka et al. [5], coauthored by members of the SRDC (Stability R&D Committee), different simulation methods and approaches for ship stability analyses and assessments were compared and discussed. The review covered, among others, intact and damage stability, regulatory issues including probabilistic approaches, advanced numerical methods for ship motion and stability failure prediction including roll damping, operational issues related to ship stability, and environmental modeling. With the advancement of computer capacity and the development of software, large models that seem to simulate the physics relatively correctly have become common. An example was given by Zhang et al. [6], who presented an analysis of the flooding process and motion responses onboard a damaged ship. The authors used the unsteady Reynolds-averaged Navier-Stokes (URANS) solver to monitor the three degrees of freedom (DOFs) of motion, investigating the effect of symmetric and asymmetric flooding on the damage stability of a ship. The volume of fluid (VOF) method was used to visualize the flooding process and capture the complex hydrodynamic behavior. Note that these methods are more suitable for single case studies, while other methods presented in Ref. [5] are preferred if a large number of simulation cases are to be studied.

1.2. Ultimate strength of damaged hull girder

During the ship design process, the concept of survivability is related to whether the ship stays afloat with sufficient reserve stability to withstand external moments, e.g., due to wind and waves. However, the reserve strength of a damaged ship girder should also be considered. Numerous papers on this subject exist in the public literature. The ISSC committee III-1 Ultimate Strength presents triennial literature reviews and benchmark studies related to the design and assessment of the ultimate strength of both intact and damaged ship structures.

In many cases in design for collision actions, prescriptive criteria derived from experience and related studies can be used. Prescriptive criteria may assume collision effects, such as the damage extent due to collision and loss of ship stability. Recently, the focus on ALS design criteria in the design requirements of different design standards has increased [1]. Greater recognition of the use of risk-based procedures to replace or support the prescriptive criteria has occurred. Different approaches are used in different design standards, the complexity of which varies. Due to the increase in computing capacity, an increasing number of advanced methods, such as nonlinear finite element (FE) analysis, are used, consequently increasing the reliability of numerical predictions and results.

In design standards, damage from accidental actions with a reasonable likelihood of occurrence should not result in the complete loss of integrity of the structure, and the load-bearing function of structures must be maintained. The design must be dimensioned such that critical parts for the overall strength are strong enough to withstand an accidental action or, alternatively, can be dimensioned to minimize the consequences with a certain redundancy without causing failure. Typically, the approaches in the design standards for these actions may be determined by either nonlinear FE analysis or energy considerations combined with simple elastic-plastic methods. Since computer resources are increasing continuously, the use of nonlinear FE analysis is becoming increasingly common.

From a reliability analysis perspective of the hull girder strength, the influence of corrosion and damage is typically studied using the Monte Carlo method. Campanile et al. [7] presented a study on a corroded bulk carrier, where a time-variant corrosion model was used to calculate the annual failure probability up to a 25-year ship lifetime. Simplified shapes of the damage openings were used to model the structural damage in the hull. The results show that corrosion and collision damage increase the probability of exceeding the ultimate strength of the hull girder capacity.

In a study presented by Parunov et al. [8], the consequence of modeling the collision damage shape on the postaccidental ultimate hull girder strength of a double-hull oil tanker was investigated. The damaged elements were removed from the FE model of the midship section of the struck ship instead of using a simplified “rectangular” shape and damage area, as recommended by the IMO [9,10]. Progressive FE analysis was carried out to calculate the residual strength index (RSI) of the damaged ship. Fifty collision scenarios were studied, and the authors concluded that near-realistic modeling of the damage shape results in a much lower failure probability of a damaged ship compared to the simplified rectangular box models proposed by the IMO [9,10]. Kuznecovs et al. [11] presented a

similar study, but they also included the effects of corrosion, deformation of the structural members around the damage opening, sagging and hogging loading conditions, and biaxial bending loading conditions. Similar to Parunov et al. [8], a near-realistic damage opening shape should be modeled to more realistically represent the ultimate strength capacity of a damaged hull girder, but the deformed structure must also be included, which can be captured only by simulation of the collision scenarios between selected candidate vessels. Since the ultimate strength analysis should be carried out for several combinations of horizontal and vertical loads (biaxial loading conditions), simplified but accurate methods are needed. Such a method was proposed by Kuznecovs et al. [11], which combines results from a few FE analyses with the advantages of the Smith method to generate accurate biaxial bending load interaction curves for different ship conditions (e.g., newly built condition, ship hull aged due to corrosion, and intact and damaged hull structures).

1.3. Objective of this study

This study extends the model development presented in Hogström and Ringsberg [12] and Schreuder et al. [13]. They proposed a decoupled simulation procedure with: (i) ship-collision simulations conducted using nonlinear explicit FE analysis to calculate the location, shape and size of the damage opening, (ii) after which this information is transferred to a ship stability code called SIMCAP that assesses the ship's dynamic damage stability conditions and time to capsize. With this procedure, realistic damage opening conditions could be included in the dynamic ship stability and flooding simulations.

The current study presents a further development of this procedure that includes ultimate strength analysis of the hull girder in the time domain, where the structural response of the ship hull girder is coupled to the motions of the intact/damaged ship. The objective is to show that time-domain-based dynamic ship motion simulations with progressive flooding should be integrated with ultimate strength calculations of the hull girder. Then, one can obtain more realistic estimations of the hull girder's structural response to ensure that it has enough reserve structural capacity under the damaged condition. The new analysis procedure and its selected methods, together with definitions of the case studies, are presented in Chapter 2. The results from the numerical simulations and analyses are presented in Chapter 3 with regard to the shape and size of the damage openings from the ship-collision scenarios, ship behavior during flooding, ultimate strength capacity and structural adequacy [14] of the hull girder against the ultimate limit state (ULS). A discussion is included in this chapter emphasizing the necessity of using the proposed methodology and its further development. Finally, in Chapter 4, the conclusions of the study are presented.

2. Methodology

The methodology and simulation procedure presented is called the SHARC model, where SHARC refers to the Swedish Transport Administration project "Structural and Hydro mechanical Assessment of Risk in Collision and grounding", under which the model was developed. A schematic of the SHARC model is presented in Fig. 1. The current study does not include a presentation of the parts of the SHARC model that refer to environmental impact and risk analysis, which are still under development.

In SHARC, accidental damage is obtained by running ship-collision simulations with the nonlinear explicit FE method; see Kuznecovs et al. [11] and Ringsberg et al. [15] for details. The location, shape and size of a damage opening are computed for each collision scenario and mapped to the SIMCAP or URSA codes (see Fig. 2). SIMCAP is a code for the simulation and analysis of dynamic ship stability conditions that was developed by Schreuder [16]; it is used for the damage stability part of the SHARC model to simulate a ship's dynamic stability behavior for both the intact and damaged conditions. The structural integrity in dynamic conditions is analyzed by URSA - a code for the ultimate and residual strength assessment of hull girders under biaxial bending loading conditions that was developed by Kuznecovs [17].

A method is developed herein to calculate the time-dependent cross-sectional forces along the length of the ship model in SIMCAP. These forces vary as a function of time due to wave action, ship motions and flooding/cargo outflow from damaged compartments and

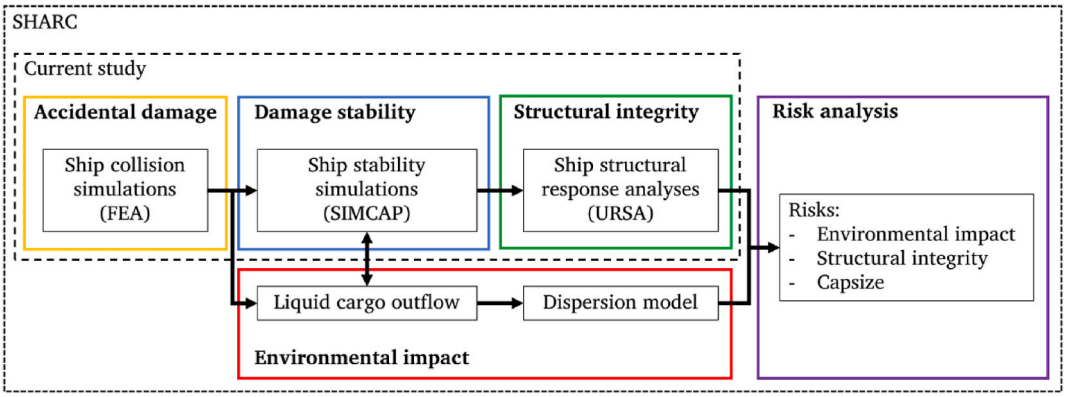

Fig. 1. A schematic of the SHARC model.

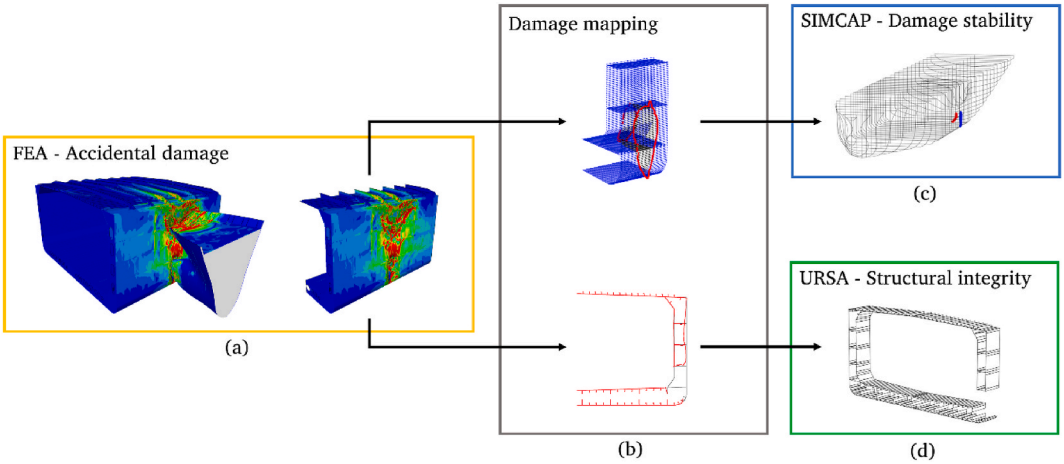

Fig. 2. (a) Results from an FE analysis of a ship-collision scenario; **(b)** mapping of the results from the FE analysis (location, shape and size of damage opening) to **(c)** SIMCAP and **(d)** URSA.

cargo holds. The structural response of the hull girder of a damaged ship is calculated and analyzed using the URSA code, presented in detail in Ref. [17]. The URSA code is updated in the current study to include the time-dependent cross-sectional forces and forces from flooded water obtained from SIMCAP. It thus enables simulation and analysis of the ultimate strength capacity of the hull girder along the length of the ship, from the instant the collision takes place before flooding starts to the end of the SIMCAP simulation, which can be, e.g., capsizing of the ship or when flooding has stopped.

With the SHARC model, the SIMCAP simulations give results referring to a ship's damage stability conditions, such as ship motions and floodwater volume. The URSA code and calculations give results such as the biaxial bending moment ULS curves of the hull girder along the length of the ship, which together with the loading history from a SIMCAP simulation can show if the ULS is exceeded and, if so, where in the hull girder. It also gives the RSI and a safety factor against the ULS defined by the biaxial loading conditions, other ship-specific conditions and collision damage.

The following sections describe the case studies investigated and the setup of the numerical simulations. The case study tanker, accident conditions and various sea states simulated are described in section 2.1. Accidental damage is acquired by running collision simulations according to the procedure in section 2.2. A description of the subsequent damage stability simulations by SIMCAP is given in section 2.3. Finally, the structural loads and ultimate strength of the damaged tanker are presented in section 2.4.

2.1. *Definition of case studies*

The parameters for the case studies were selected to showcase the features of the SHARC methodology for collision scenarios and for structural and environmental conditions that are both reasonably realistic and representative. The studied damage cases stem from ship-to-ship collisions between two similar-sized vessels. The struck ship was a coastal double-hull oil tanker carrying cargo in 12 tanks in starboard-port-side pairs, and the striking ship was a chemical product tanker with a total displacement of 10,800 tonnes. The cargo hold arrangement and hull lines of the struck tanker are shown in Figs. 3 and 4, respectively. The principal particulars of the ship are summarized in Table 1.

To assure progressive flooding and a structural condition regarded as critical from the ULS perspective, the collision impact was

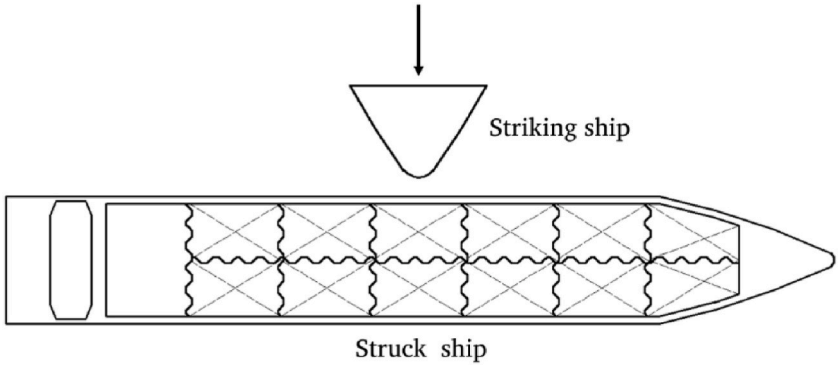

Fig. 3. Collision setup and cargo hold arrangement of the struck tanker.

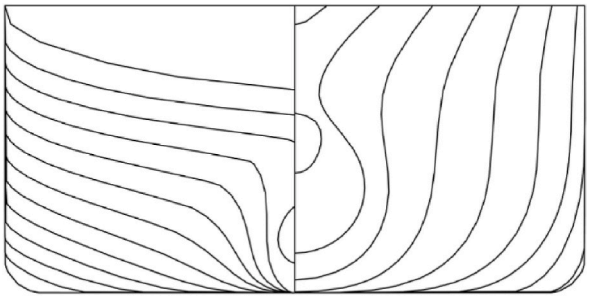

Fig. 4. Body plan representation of the struck tanker's hull lines.

Table 1
Principal particulars of the struck tanker.

Parameter	Value	Units
Length overall, LOA	139.9	m
Length between perpendiculars, LPP	134.0	m
Breadth, B	21.5	m
Draft, T	7.4	m
Longitudinal center of gravity, LCG	69.3	m
Center of gravity, KG	5.0	m
Deadweight, DWT	11,500	tonnes
Total displacement	16,200	tonnes

amidships, between transverse bulkheads and web frames, while the relative draft of the vessels was selected with both keels aligned. An impact at the selected position will result in an opening exposing liquid cargo holds to sea water and a drastic reduction in ultimate strength at a location where maximum hull bending moments are usually attained. The collision impact was set at a 90° angle and an initial speed of 5 knots. This low-speed, right-angled collision with an idle vessel amidships is a representative accident justified by collision statistics and probabilistic impact scenario models [18–20]. For instance, analyses of collision statistics by Brown [20] revealed that a striking ship's speed is lower than a ship's service speed due to actions taken just prior to the collision, and is typically around 5 knots which is a representative maneuvering speed according to Rawson et al. [18]. It was also shown in Ref. [20] that struck ships are frequently moored or at anchor which explains most probable speed of zero knots and validates the assumption of an idle struck ship. Moreover, the most probable collision angle resulting in substantial damage according to reported collision accident statistics is of 90° [20]. Finally, the collision location amidships in general and for tankers specifically is congruent with the conclusions in Lützen [19]. The effects of the collision angle, location and speed on the structural crashworthiness of ships were previously investigated in Ringsberg et al. [21], Baxevanis [22] and Kuznecovs et al. [11], respectively.

Two structural conditions were applied in the FE and URSA models of the struck tanker: newly built and with structural degradation. The degradation or aging of the oil tanker was represented by corrosion with increased friction coefficients [21] and corrosion wastage according to Harmonized Common Structural Rules for Bulk Carriers and Oil Tankers (CSR-H) [23] with a full corrosion margin reduction. In addition, stress concentrations on the plate surfaces due to local pit corrosion were considered by altering the material properties depending on the degree of corrosion degradation according to Garbatov et al. [24]. The sophisticated corrosion modeling approach was proposed by Ringsberg et al. [15], and the negative effect of corrosion on structural safety was shown by Kuznecovs et al. [11].

Dynamic ship stability simulations in SIMCAP were carried out for a set of sea state conditions. The setup consists of simulations of the intact ship and of the two damage cases in headings from 0° (following seas) to 315° in 45° increments. Regular wave heights of 1, 2, 3 and 6 m and a wavelength equal to the length of the ship, corresponding to a frequency of 0.663 rad/s, were used in the simulations. Still water simulations were also carried out as references. The duration of the simulations was 5–10 min in real time to ensure that a steady state was reached for the damaged cases.

Table 2
Nomenclature for the description of the case studies.

Parameter	Value	Notation
Vessel type	Tanker	T
Structural degradation	As-built	1
	Corroded	5
Structural damage	Intact	I
	Damaged	D
Heading	[deg]	WD [deg]
Wave height	[m]	H [m]

All simulation cases are denoted according to Table 2. For example, T-5-D-WD45-H3 denotes a corroded tanker with collision damage subjected to quartering waves approaching 45° with a wave height of 3 m. Note that H0 indicates the absence of waves, i.e., still water conditions.

2.2. Ship-collision simulations by FEA

Estimation of the damage opening size and shape is necessary for damaged stability calculations and an assessment of the ship's structural residual strength. In damage stability simulations, the size and location of the opening will determine the flooding process. In the assessment of the hull structural integrity, accurate modeling of the damage is advantageous since simplification of the opening shape and omission of the damage to the surrounding nonfractured structural members may result in overprediction of the hull's residual bending strength [11]. This chapter presents a general description of how the ship-to-ship collision damage was obtained. Details of the structural models and collision analysis setup are available in Refs. [11,15]. In the following, only a brief summary is outlined.

Structural damage to the hull of the struck tanker was obtained with explicit nonlinear FE collision simulations in Abaqus/Explicit version 6.13–3 [25]. Fig. 5 shows the setup of the collision simulations and internal structural arrangement of the vessels involved. The striking tanker was represented by its deformable bulbous bow section with an attached point mass corresponding to the total displacement of the vessel. The struck tanker was modeled with its parallel midship body composed of seven transverse sections that were sufficiently long to accommodate the largest damage possible and minimize influence from the fixed boundary conditions at its respective ends. Since the collision process is a quick event involving two similar-sized vessels with large masses, the global dynamics of the vessel and its motions may be assumed to have a minor influence on the resulting damage opening, and the applied fixed boundary conditions can be considered reasonable.

FE models of the vessels comprise three- and four-node shell elements with reduced integration (S3R/S4R) and five section points through the thickness. A mesh convergence analysis resulted in an element size of 60 mm. To model the contact between plate surfaces during collision, the general contact condition with surface friction coefficients was applied. For both vessels, a nonlinear constitutive model based on the elastic-plastic power law with isotropic hardening was applied. The model incorporates strain-rate dependency with the Cowper-Symonds relation and damage initiation and evolution models for predicting material degradation leading to failure.

A collision simulation starts with a release of the striking bow section assigned an initial velocity and restricted to moving in a prescribed right-angle collision direction. During impact, the kinetic energy of the bow is absorbed elastically and dissipated through surface friction, plastic deformations and fracture during stretching, crushing and tearing - predominant failure modes of the structural members. The damage is regarded as fully developed and the collision simulation as finished when the indenter's speed reaches zero knots. Some of the elastic energy may be restored and translated to the bow, resulting in a "bounce back" motion, but it is not relevant to the structural damage estimation.

2.3. Ship stability simulations in SIMCAP

The simulation tool SIMCAP presented by Schreuder [16] is based on a hybrid approach where the hydrodynamic radiation and diffraction forces are based on linear strip theory and are expressed in the time domain through the impulse response function concept detailed in Cummins [26]. The excitation forces from the incident wave are treated nonlinearly through body-exact pressure integration over the wetted hull surface, where the pressure is defined as the sum of linear dynamic and hydrostatic pressure as suggested by Faltinsen [27]. The latter enables retaining all hydrostatic stability properties of a damaged ship subjected to flooding. The impact of viscous effects on roll damping can be treated as quadratic damping, where the damping coefficients are determined through model experiments.

Flooding of a damaged ship is treated as a quasi-stationary process with a versatile and robust damage opening definition and the inclusion of floodwater inertia in the equations of motion. The shape, size and location of a damage opening are calculated in this study using FEA, as presented in section 2.2. The damage opening is defined in SIMCAP through a grid of points (see Figs. 2 and 11), which matches exactly the mapping from the FEA. The fluid flow through each grid point is determined through a formulation based on the Bernoulli equation. The behavior of flooded water is based on quasistatic assumptions, where the floodwater surface is horizontal. The floodwater affects the ship's motions through its weight and inertia. The damage opening areas in the inner and outer shell are

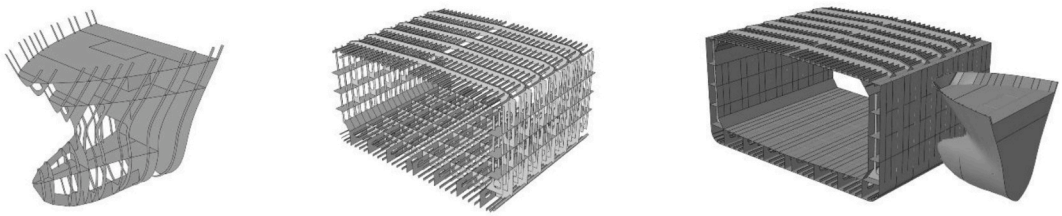

Fig. 5. Internal structural arrangement of **(a)** the striking bow, **(b)** midship section of the struck tanker, and **(c)** collision setup.

considered separately for correct estimation of the progressive flooding and damaged stability when different compartments lost their integrity. While an opening in the outer shell defines the exchange of outboard and ballast waters, an inner opening determines flooding of the cargo holds and the inflow and outflow of liquid cargo.

The SIMCAP code is updated in this study to output the ship motions and cross-section forces needed for the structural response analyses of the hull girder presented in section 2.4. The forces include effects from the incident wave and wave diffraction together with the radiation forces due to ship motions. In the present study, the heave, pitch and roll motions are simulated, while sway and yaw are captive. In the damage simulations, the floodwater volume and corresponding center of gravity are also output by SIMCAP. The radius of gyration in pitch for an intact ship is set to 0.27 × LOA, and a discharge coefficient of 0.6 is used in the flooding simulations (see Refs. [16,28]).

2.4. Ship structural response analyses in URSA

The SHARC methodology includes a structural safety assessment of a ship hull subjected to dynamically varying environmental and loading conditions. The structural safety of a ship is judged from a comparison of the loads acting on a hull – demand D – and the hull's ultimate strength – capacity C. A structure is regarded as safe when the structural adequacy measure, defined according to Eq. (1) [14], is less than 1.0, i.e., the demand does not exceed the ultimate strength or the maximum load carrying capacity.

$$\eta = \frac{D}{C} \tag{1}$$

To calculate the demand, a set of forces is considered: radiation, wave diffraction, incident wave pressure, gravity and inertia. The former three forces are obtained by SIMCAP simulations together with the time history of the ship's motions and the mass distribution of flooded water across the flooded compartments (see section 2.3). Both gravitational and inertial forces are considered from arbitrary (linear/nonlinear) mass distribution and vessel accelerations. Due to the lack of detailed information on the mass distribution along the case study ship, the total mass of the ship is assumed to be linearly distributed to match the LCG.

The shear forces and bending moments are calculated by integrating the cross-sectional forces with respect to the hull's longitudinal x-direction (see Fig. 6). Two components of the integrated bending are considered: vertical M_V and horizontal M_H bending moments about the y- and z-axes of the ship's local coordinate system, respectively. The longitudinal position of the instantaneous maximum bending moment and its biaxial components are found for every SIMCAP simulation time series for further comparison with the available hull strength capacity.

The ULS of a ship structure is determined by the ultimate strength or capacity of its hull to sustain applied loads. In the current study, the hull girder's ultimate strength in longitudinal bending is considered the most critical. This consideration implies that both demand and capacity are defined for pure bending moments when the shear forces are zero, which corresponds to the bending moment peak values.

The ultimate strength can be obtained with high-fidelity FE simulations of hull girder bending, but the time and effort required are high. A rapid assessment of the ultimate strength can be carried out by applying the Smith method [29], a well-established approach for progressive collapse analysis of symmetrical hulls in vertical bending recognized by many classification societies [23,30,31]. Fujikubo [32] modified the Smith method to enable progressive collapse analysis of asymmetric cross-sections in biaxial bending conditions. The flaw of the simplified methods is loss of accuracy due to the assumptions and idealizations they are based on. To enhance the efficiency of the calculations and preserve good accuracy simultaneously, a calibration method using a curve fitting procedure proposed by Kuznecovs et al. [11] is applied to make use of as few FEAs as possible to generate correction factors for the results of the modified Smith method. According to the procedure, the minimum number of FEAs required to obtain reliable correction factors is 7 and 12 for intact and impact damaged cases, respectively. This method is implemented in an URSA code that can be used for bending ultimate and residual strength assessments.

The biaxial bending ULS capacity of the tanker's hull girder under different structural conditions is represented by interaction curves on a polar diagram (see Fig. 7). The interaction curves define the ultimate strength of a ship hull under various combinations of vertical and horizontal bending moments. According to Ref. [11], the calibrated interaction curves for all four structural conditions of the studied tanker can be expressed by Eq. (2) [33], where M_V and M_H are coordinates on the capacity curve, M_{UV} and M_{UH} are the ultimate vertical and horizontal bending moments in the ship's local coordinate system, respectively, and β is a shape factor. The respective equation coefficients presented in Table 3 are unique for each quadrant Q_i on a biaxial polar diagram.

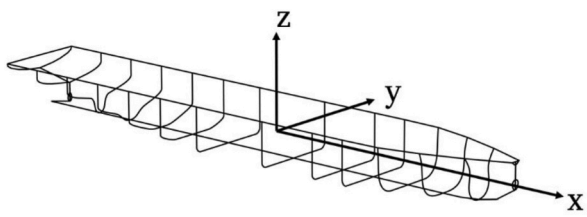

Fig. 6. Definition of ship's local coordinate system.

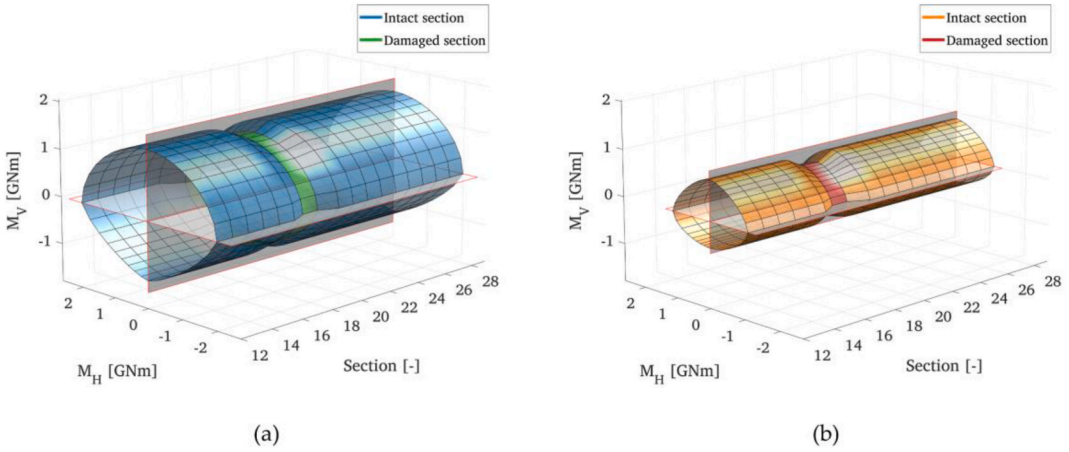

Fig. 7. Biaxial polar diagram with capacity interaction curves of the parallel midship section for all four structural conditions defined according to Table 2.

Table 3
Coefficients of interaction equations for all four structural conditions; see Ref. [11] for details. Q_i indicates quadrant number (i = 1, 2, 3 or 4), where Q_1 corresponds to bending moment loading ratios between 0° and 90° on the biaxial polar diagram.

Case	Coefficient	Q1	Q2	Q3	Q4
T-1-I	M_{UH} [GNm]	1.98	−1.98	−1.98	1.98
	[GNm]	1.56	1.48	−1.22	−1.22
	β [−]	1.85	1.85	1.33	1.33
T-5-I	M_{UH} [GNm]	1.12	−1.12	−1.12	1.12
	M_{UV} [GNm]	0.87	0.87	−0.54	−0.54
	β [−]	1.50	1.50	1.69	1.69
T-1-D	M_{UH} [GNm]	1.66	−1.81	−1.81	1.66
	M_{UV} [GNm]	1.29	1.29	−1.01	−1.01
	β [−]	1.90	1.85	1.56	1.52
T-5-D	M_{UH} [GNm]	0.78	−0.86	−0.86	0.78
	M_{UV} [GNm]	0.68	0.68	−0.45	−0.45
	β [−]	1.80	1.46	1.69	1.53

$$\left(\frac{M_V}{M_{UV}}\right)^{\beta} + \left(\frac{M_H}{M_{UH}}\right)^{\beta} = 1 \tag{2}$$

A common practice for the ultimate and residual strength assessment of ships is to check whether any transverse section of an intact or damaged ship will be able to sustain a predefined vertical bending load [23]. Indeed, the ultimate capacity of a hull may vary with its length due to local accidental damage openings, nonuniform hull forms or structural arrangements. However, the maximum

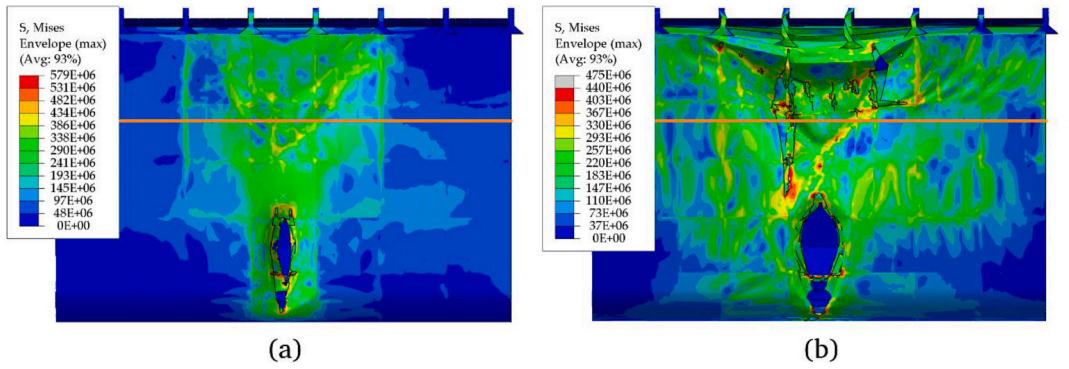

Fig. 8. Capacity surfaces for parallel midship bodies of the **(a)** T-1-D and **(b)** T-5-D cases with local collision damage (marked in green and red, respectively). (For interpretation of the references to colour in this figure legend, the reader is referred to the Web version of this article.)

bending moment may have both vertical and horizontal components and be applied at different sections as a result of broad spectra of acting time-varying loads. In the rules, this problem is dealt with by using partial safety factors; while this approach is convenient from an engineering perspective, it does not fully reflect the actual processes, and misleading results may be obtained. In addition, some unfavorable loading conditions may be overlooked if only a specified range of predefined loads is considered during structural design. The consequences of this may be rather dramatic, with the MSC Napoli accident being a prime example [34]. Thus, to enhance the accuracy of structural safety assessments, the URSA code was further developed to include a comparison of the actual structural capacity – ultimate bending strength – with the actual demand – biaxial bending load imposed on the most loaded sections.

For that purpose, a three-dimensional bending moment capacity surface representing a longitudinally varying biaxial bending strength was proposed in this study. The capacity surface is confined by points on the interaction curves depicting the biaxial bending strength of the respective section. The shape of the capacity surface of an intact prismatic hull girder remains unchanged with its length. However, local damage negatively affects the ultimate strength of the girder, and its capacity surface is disturbed locally between sections 18 and 19, as shown in Fig. 8. Thus, the risk of capacity excess by the applied loads is increased; see section 3.3. The critical location and point in time at which the ULS is reached can be elicited by plotting the bending load time series as trace lines against the capacity surface. A structure is regarded as failed when any point on the trace line is outside the capacity surface boundaries.

The applied approach for determining the overall structural safety was inspired by the Dang Van criterion used for multiaxial high cycle fatigue assessment [35]. In this study, structural safety is quantified by the structural adequacy measure η (Eq. (1)) and calculated for all bending moment time series in the respective section. The demand D is defined as the instantaneous total bending moment, and the capacity C, as the distance from the origin to the point on the capacity surface closest to the demand (see Fig. 9). Structural adequacy is assumed to be represented by the worst condition; for every section, i is found as $\eta_s^i = max(\eta(i))$, and for the whole vessel, $\eta_v = \max(\eta_s)$.

3. Results

This chapter presents the obtained collision damage openings in section 3.1. The results from damage stability simulations together with force analyses for varying sea states are given in section 3.2. Finally, structural safety assessments are presented in section 3.3, and the results are discussed in section 3.4.

3.1. Damage shape and size

The FE collision simulations resulted in two damage openings with different shapes and sizes. The shapes are shown in Fig. 10. The resulting collision energy shares, indenter penetration depths and damage sizes are summarized in Table 4. The size of the damage was quantified by the projected area of the opening on undeformed plans of the inner and outer plating.

The structural deformation and energy dissipation in both cases corresponded to the shared-energy design [36]. The shares of the internal energies were approximately 20–30% and 60% for the indenter and the struck hull, respectively. The collisions resulted in a large contact area between the bow and the side-shell structure and extensive plastic deformation in the forecastle structure of the

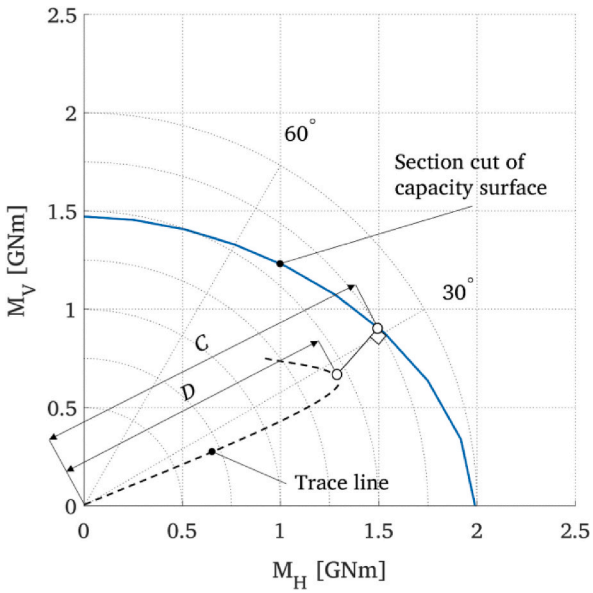

Fig. 9. Definition of the demand and capacity values.

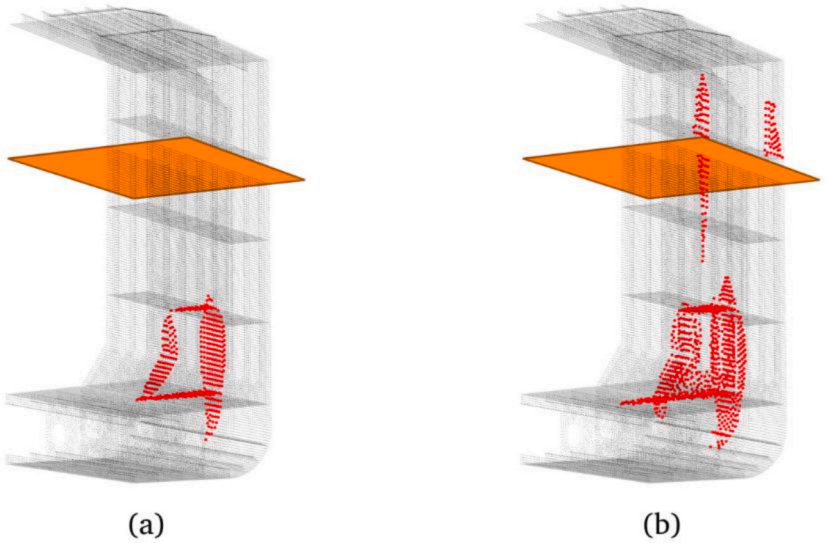

Fig. 10. Collision damage patterns and stress distributions in [Pa] for cases **(a)** T-1-D and **(b)** T-5-D. The orange line marks the design water level. (For interpretation of the references to colour in this figure legend, the reader is referred to the Web version of this article.)

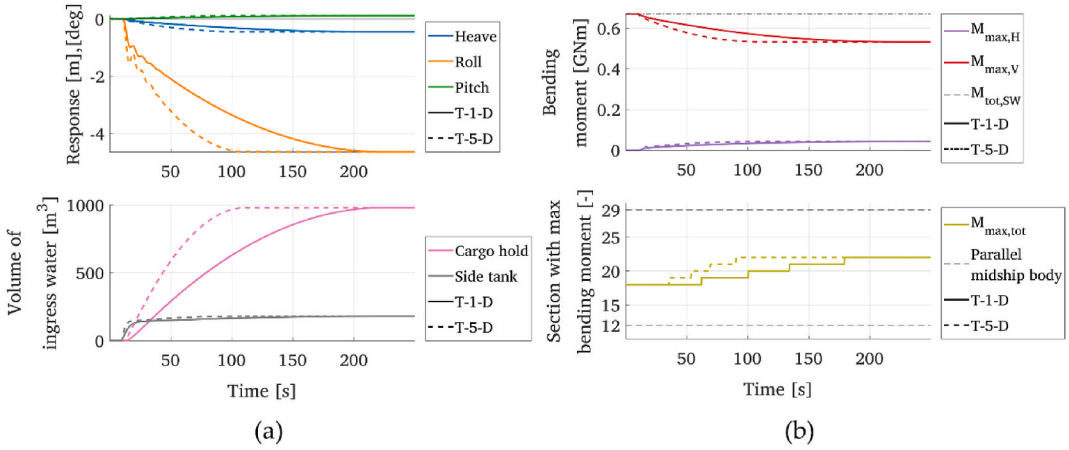

Fig. 11. Mapping of damage openings (in red) in the SIMCAP damage stability simulations for the **(a)** T-1-D and **(b)** T-5-D cases. The orange plane marks the design water level. (For interpretation of the references to colour in this figure legend, the reader is referred to the Web version of this article.)

Table 4
Summary of the collision simulation results.

Parameter	T-1-D		T-5-D	
Projected damage opening area [m^2]	Inner shell 1.8	Outer shell 4.2	Inner shell 2.8	Outer shell 8.8
Internal energy, bow [%]	29		22	
Internal energy, hull [%]	56		58	
Frictional dissipation [%]	15		20	
Penetration depth [m]	2.6		3.6	

striking bow. Two types of damage to the struck hull may be distinguished: a damage opening below the waterline near the bilge due to penetration of the very stiff bulbous bow and damage to the upper part of the side plating due to contact with the forecastle. The area of the opening in the bilge corresponded approximately to the cross-sectional area of the bulbous bow at a certain penetration depth [11].

For the corroded case, the results show a drastic increase in the damage opening area despite a larger portion of energy being

dissipated by friction due to the increased friction coefficients of the corroded plating. In addition, the penetration depth of the striking bow was larger since the structure was weakened due to the loss of corrosion margins and changes in the material properties, which resulted in extensive damage to the upper part with crack-shaped openings and shear buckling of the surrounding outer side plating. The presence of this damage in the vicinity of an opening together with the residual stresses caused by plastic deformations will negatively affect the structural stability of the hull [11].

3.2. Ship stability simulations and force analyses

The damage obtained by the FE collision simulations in section 3.1 was mapped to SIMCAP models, as shown in Fig. 11, according to the procedure described in section 2.3. This damage resulted in a breach of the watertight integrity of one side of the water ballast tank and one of the cargo holds, which were both assumed to be empty at the time of collision.

Fig. 12a presents the results of SIMCAP simulations for still water conditions of the two damaged hulls T-1-D and T-5-D. The results show that after fully developed flooding, both cases are identical from a hydrostatic point of view: an equilibrium heel angle of 4.6°, an increase in draft of 0.45 m and a forward trim of 0.3 m. The slight forward trim is attributed to the almost amidship location of the damaged cargo hold.

The development of the floodwater volume in the damaged compartments is shown in Fig. 12a. The damage openings are assumed to appear 10 s into the simulations, after which rapid flooding of the side tank occurs, which in turn results in rapid list (roll) development, where some transient, dynamic roll behavior can also be seen. Because the damage opening between the side tank and cargo hold becomes submerged after a couple of seconds, most of the floodwater entering the ship floods into the cargo hold, and the flood rate in the side tank is reduced. For both the as-built and corroded struck tankers, collision caused damage that involved the same two internal compartments (see Fig. 11) and resulted in similar floodwater volumes and distributions. However, the corroded tanker reached the steady state faster due to the larger damage opening area: after approximately 3 and 2 min for the T-1-D and T-5-D cases, respectively.

Because the hydrostatic equilibrium conditions are identical, both damaged hulls experience the same loads after flooding. Fig. 12b shows the development of the horizontal and vertical components of the maximum bending moment with time. Initially, the intact tanker is subjected to a still water bending moment of 0.67 GNm in hogging. After the introduction of damage, a transition from the pure vertical to biaxial bending conditions is observed due to the development of a list, subjecting the damaged portside of the hull to compressive loads. In addition, lost buoyancy, represented by an increase in weight of the breached compartments, located at sections 14 and 22 (see Fig. 13), reduces the total bending moment down to 0.53 GNm. Another consequence of the extra weight is load redistribution due to trim that caused forward shift of the maximum bending moment onset location.

When subjected to waves, the motion responses of a vessel and the resulting bending loads are cyclic and depend on the damage conditions, wave characteristics and encountering direction. Because of the approaching waves and vessel motions, different portions of the damage opening are exposed to sea water, affecting the inflow and outflow rates. Thus, more time is required for the flooding process to finish and the vessel to attain its dynamic steady state. Comparing the still water and high seas conditions, the flooding durations increase from 3 to 8 and from 2 to 3 min for the T-1-D and T-5-D cases, respectively. Note that the effect of the wave-encountering direction on the flooding duration is minor. For the still water conditions, the flooding process of the damaged corroded hull is reaffirmed to be more rapid due to the larger opening area.

In addition to flooding duration, no other significant differences in the motions and resulting forces were observed between the two damaged hulls, as in both cases, the watertight integrity of the same internal compartments was breached. Moreover, the vessel amplitudes in response to regular waves have a close to linear correlation with the wave height. Thus, the results from the SIMCAP flooding process simulations are studied in detail by examining the damaged T-1-D tanker subjected to waves with a wave height of 6

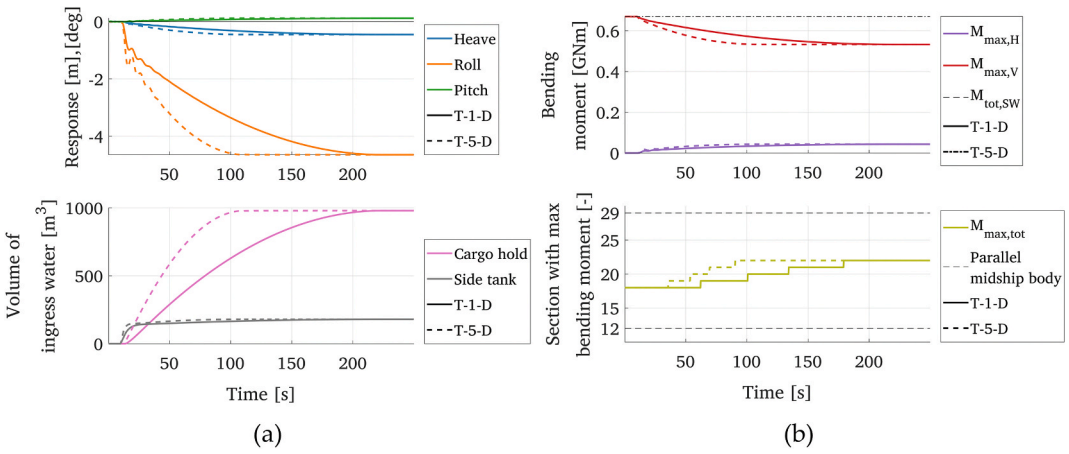

Fig. 12. (a) Motion response and floodwater volume, and **(b)** bending moment load histories of the flooding process for damaged T-1-D (solid line) and T-5-D (dashed line) hulls under still water conditions.

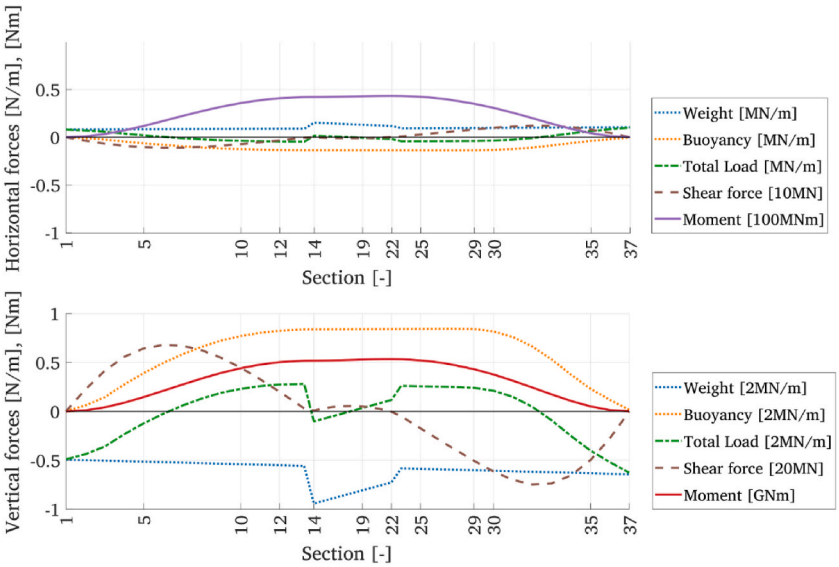

Fig. 13. Distribution of forces along the damaged hull after flooding in still water conditions.

m.

The results for the tanker subjected to head and beam waves are presented in Figs. 14 and 15, respectively. Here, collision damage is introduced 50 s after the simulation start time to ensure steady-state motions of the initially intact vessel. From Fig. 14a, the head waves acting on the intact vessel clearly predominantly give rise to pitch and heave oscillations. These conditions force cyclic loads in pure vertical bending with a mean value corresponding to a still water moment of 0.67 GNm and an amplitude of 0.36 GNm. The onset location of the maximum moment is no longer steady and changes between frames 13 and 28 (see Fig. 14b).

When a damage-induced opening is introduced to the hull, portside list and cyclic roll motions develop with increased floodwater volume. For still water conditions, the total bending moment is reduced as the floodwater volume increases. Moreover, the horizontal bending component rises together with the roll motions, and the loading conditions become biaxial. With increased pitch motions, the onset location of the maximum bending moment becomes widespread but maintains its position within frames 12–29, corresponding to the parallel midship body of the tanker.

While the horizontal bending moment component is of less importance in head waves, it may constitute 40–50% of the total bending load during operation in beam seas when rolling is the dominant response with very excessive cyclic motions (see Fig. 15). Contrary to the head waves, reduced pitch and heave motions in the beam seas resulted in a reduced amplitude of the cyclic vertical bending moment and a narrower span of the maximum moment onset locations (Fig. 15b).

The observed trends are also supported by Figs. 16 and 17, where cyclic motions and loads for different wave-encountering directions are presented as the mean and amplitude values for the T-1 tanker under the intact and damaged conditions, respectively. For

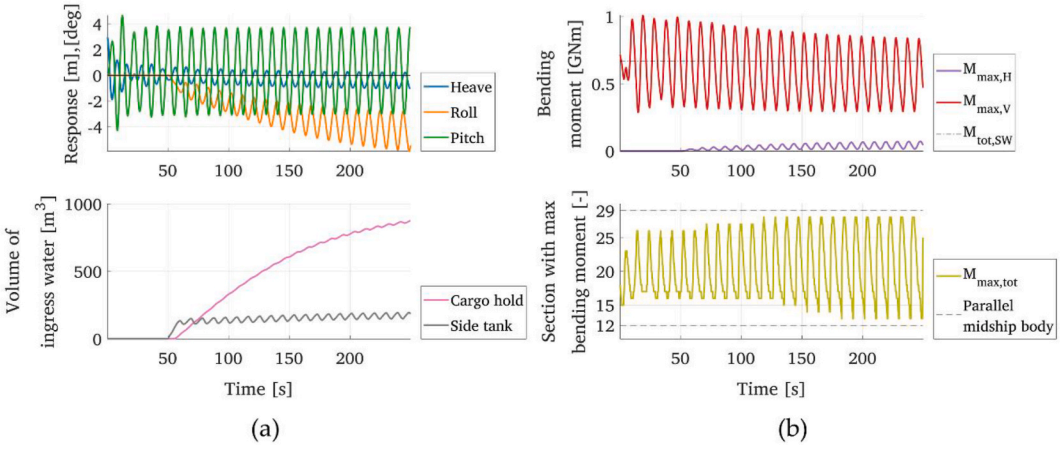

Fig. 14. (a) Motion response and floodwater volume, and **(b)** bending moment load histories of the flooding process for the T-1-D-WD180-H6 case: tanker with as-built scantlings and collision damage subjected to head waves of 6 m in height.

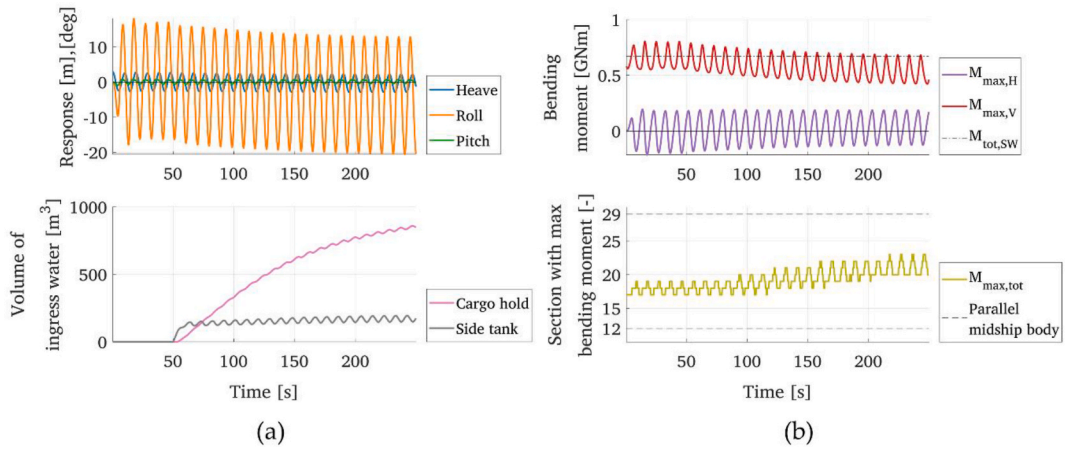

Fig. 15. (a) Motion response and floodwater volume, and **(b)** bending moment load histories of the flooding process for the T-1-D-WD90-H6 case: tanker with as-built scantlings and collision damage subjected to starboard side beam waves of 6 m in height.

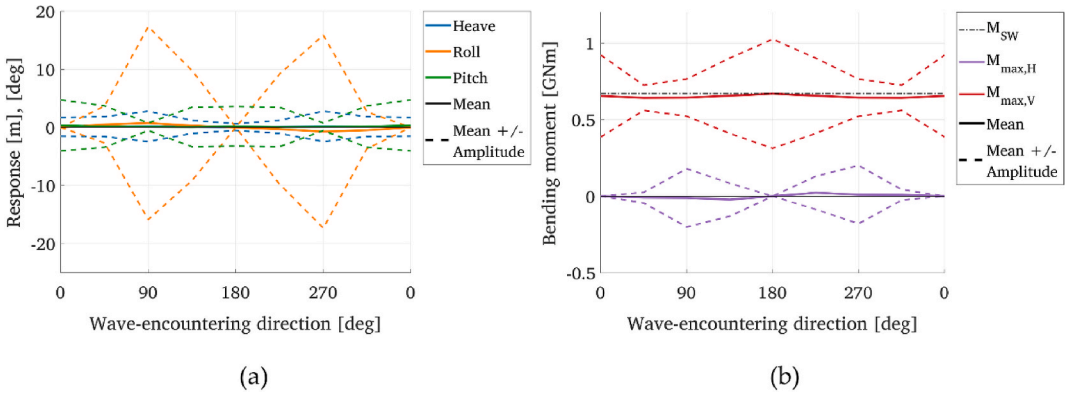

Fig. 16. Mean (solid line) and amplitude (dashed line) of the **(a)** motion response and **(b)** bending moment load components as a function of the wave-encountering direction for intact tanker T-1-I subjected to 6 m waves.

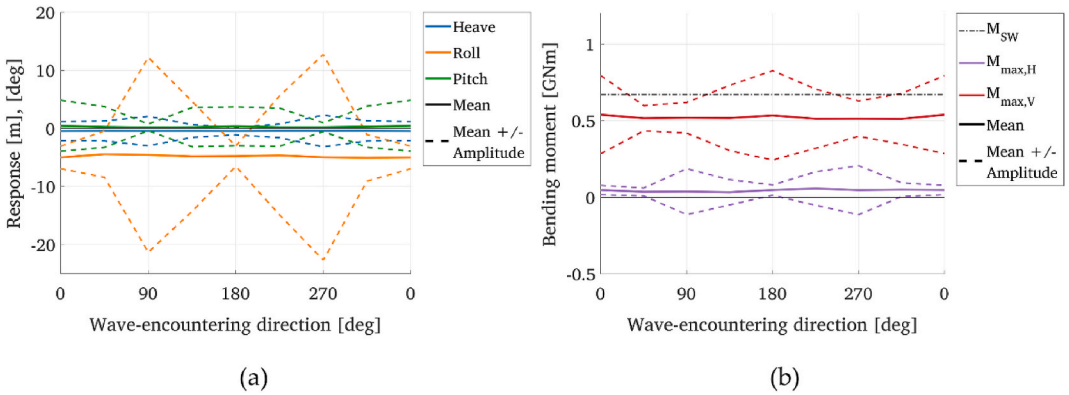

Fig. 17. Mean (solid line) and amplitude (dashed line) of the **(a)** motion response and **(b)** bending moment load components as a function of the wave-encountering direction for damaged tanker T-1-D subjected to 6 m waves.

both vessels, large pitch motions are predominant in the head or following seas, contributing to large oscillations in the vertical bending moment and a wide spread of the loading onset locations. When a vessel is subjected to beam waves instead, the pitch and vertical bending moment amplitudes are reduced, and the loads act within a narrow span amidships. Concurrently, responses in the beam seas are characterized by excessive roll motions, and large amplitudes of the horizontal bending are observed. The heave motions

are also their largest for beam seas when the vessel is aligned with the wave front. A summary of how the motions and amplitudes of the bending load components are correlated with the wave-encountering direction is presented in Table 5.

From Fig. 17a, flooding clearly results in a list or shift of the mean roll angle, with deviations depending on the side from which the waves approach the vessel. Loss of buoyancy leads to a reduced mean of the total bending moment and the accompanying list with a simultaneous increase in its horizontal component (see Fig. 17b).

3.3. Structural safety analyses

From the investigation of motions and loads in various conditions and environments, consideration of the biaxial bending is clearly necessary for correct estimation of the structural safety if a vessel has a heel or list angle or a combination of both. In addition, since the longitudinal location of a maximum load is transient during wave action, the safety of a structure may not be estimated realistically from the examination of the midship section capacity alone. With this reasoning, structural safety assessments in this study are carried out in accordance with the procedure proposed in section 2.4, where the demand history from bending loads is plotted and compared against the ultimate strength capacity surface to obtain the structural adequacy of a ship.

From the force analyses, the maximum bending loads always act within the parallel midship body for the selected case studies. Therefore, the ultimate strength is obtained for sections 12 to 29 of the tanker. For intact hull T-1-I, the capacity surface is constant along the length of its prismatic body and symmetric about the vertical M_V - x plane (see Fig. 18). Clearly, the trace lines, representing the time series of the instant bending moment, are in the vertical plane for the head and following waves. When a vessel is subjected to roll motions in the beam seas, the trace lines are three-dimensional due to biaxial bending, shown as ellipses on the biaxial plot in Fig. 18. Note that the trajectories of all trace lines have a closed profile because of the steady-state conditions they are representing. In all cases, the maximum loads act at sections 17 and 18 close to the midship, and the margin between the capacity surface and trace lines is substantial. This example may be considered confirmation that the strength assessment of the midship section of an intact as-built vessel against prescribed vertical bending loads is adequate.

However, both the capacity surface and demand histories are altered when collision damage is introduced (see Fig. 19). The damage results in locally reduced ultimate strength. Thus, the capacity surface is disturbed across the damaged sections, and symmetry about the vertical plane cannot be maintained. Furthermore, progressive flooding due to the damage opening affects the vessel orientation, motions and weight distribution. For this case, the trace lines have different trajectories and are three-dimensional for all wave-encountering directions. Namely, a vessel with asymmetric damage is always subjected to biaxial loading conditions. The safety margin between the trace lines and capacity surface increases for all sections except the damaged one, owing to a decrease in the hogging moment, as discussed in section 3.2.

The ultimate strength of the T-5 tanker suffering from severe corrosion damage is further reduced. The reduction is nonuniform because the corrosion intensity depends on, among other factors, the location and orientation of plate members within the structure. In addition, corrosion negatively affects the crashworthiness of a ship and leads to increased structural damage (see Figs. 10 and 11). While corrosion results in an overall reduction in the strength along the midship body, the combination of both corrosion and collision impact leads to a drastic local decrease in the ultimate capacity of the structure (see Fig. 20). The trajectories of the load trace lines indicate that the structure is subjected to biaxial bending. The capacity is exceeded in the head and following seas at damaged sections 18 and 19. Assuming identical bending loads and collision impact located at sections 21 to 23 instead, i.e., closer to the bow, the most dangerous condition would be attained with beam waves approaching from the breached port side.

The safety of the tanker is assessed by the structural adequacy measure η obtained according to section 2.4, the results of which are presented as polar diagrams in Fig. 21 for all sea states with wave heights ranging between 1 and 6 m, see section 2.1. A structural adequacy value larger than 1 indicates dangerous conditions when the ultimate strength of a vessel is exceeded. In general, the η value clearly increases with increasing wave height. Another common feature for all cases is that most unfavorable conditions are found in the head or following seas when vertical bending prevails.

For intact cases T-1-I and T-5-I, maximum structural adequacy is attained in the head waves. While the T-1-I tanker (Fig. 21a) with as-built scantlings has an adequate safety margin for all the sea states studied, the structural capacity of the corroded T-5-I tanker (Fig. 21c) is insufficient when subjected to head or following waves of 4.6–5.3 m in height, respectively. Furthermore, headings of 0° and 115°–245° should be avoided in high seas.

The symmetry of the polar diagrams about the vertical axis is violated for damaged vessels due to both biaxial bending and asymmetric damage. For the T-1-D case, the reduction in the hogging moment due to buoyancy loss is reflected by the lower adequacy

Table 5
Summary of the motion response and acting bending load amplitudes due to different wave-encountering directions.

	Head or following seas	Beam seas
Heave	Low	High
Roll	Low	High
Pitch	High	Low
M_H	Low	High
M_V	High	Low
Spread of onset location	High	Low

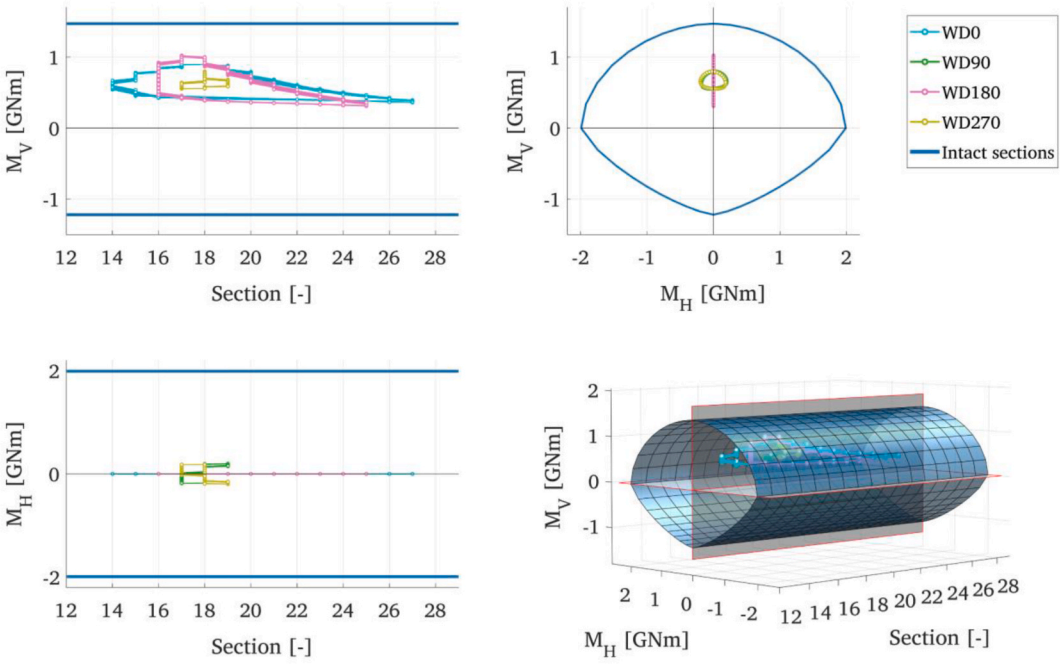

Fig. 18. Demand-capacity plot for the T-1-I tanker acting in waves of 6 m in height.

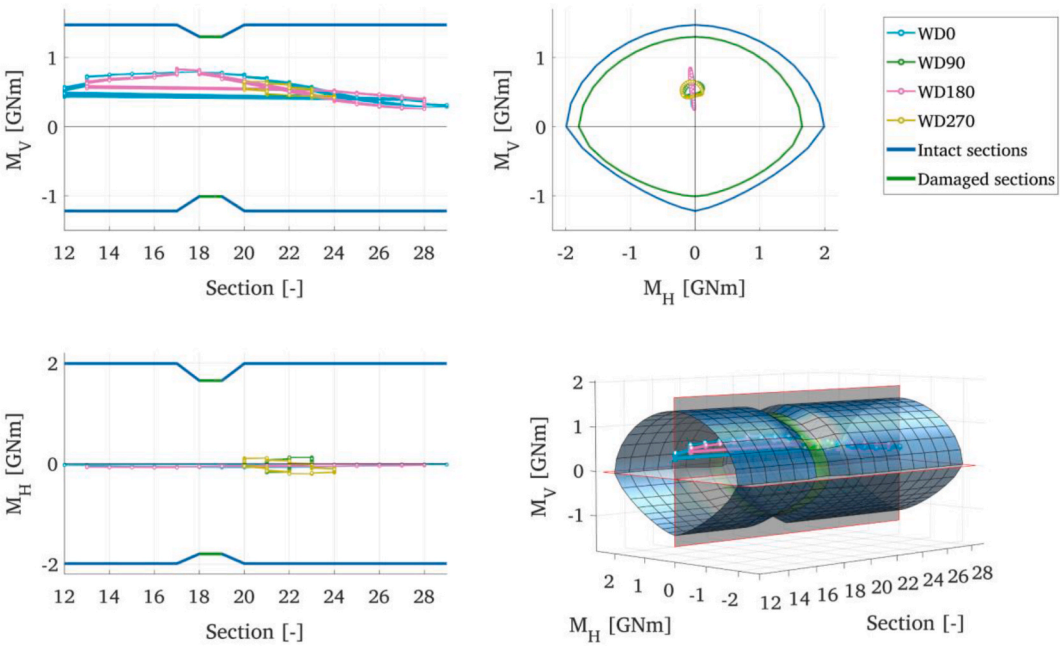

Fig. 19. Demand-capacity plot for the T-1-D tanker acting in waves of 6 m in height.

η for all wave-encountering directions (see Fig. 21b). However, for the corroded T-5-D tanker with collision damage (Fig. 21d), a safety margin gain due to redistribution of the loads caused by flooding is observed only for the bow, beam and quartering seas. Still, compared to the intact case of T-5-I, the ULS in the head seas is reached earlier, at a wave height of 3.7 m. A minor effect of the transverse location of the damage, i.e., on either the port or starboard side, is observed: η is slightly increased in the bow and decreased in the beam waves approaching from a direction opposite the damaged side.

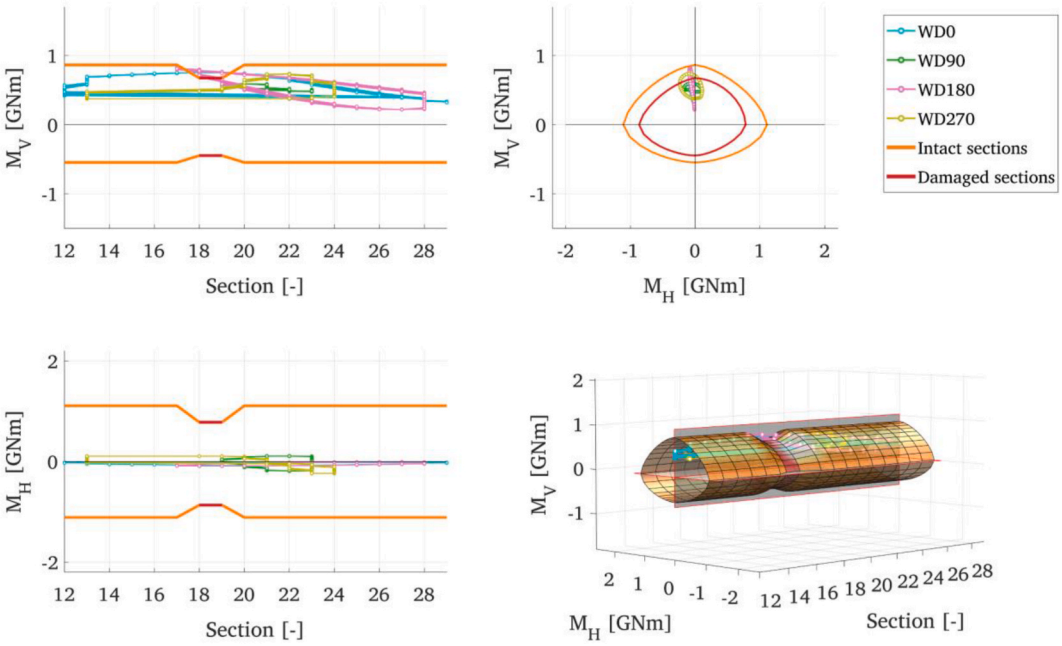

Fig. 20. Demand-capacity plot for the T-5-D tanker acting in waves of 6 m in height.

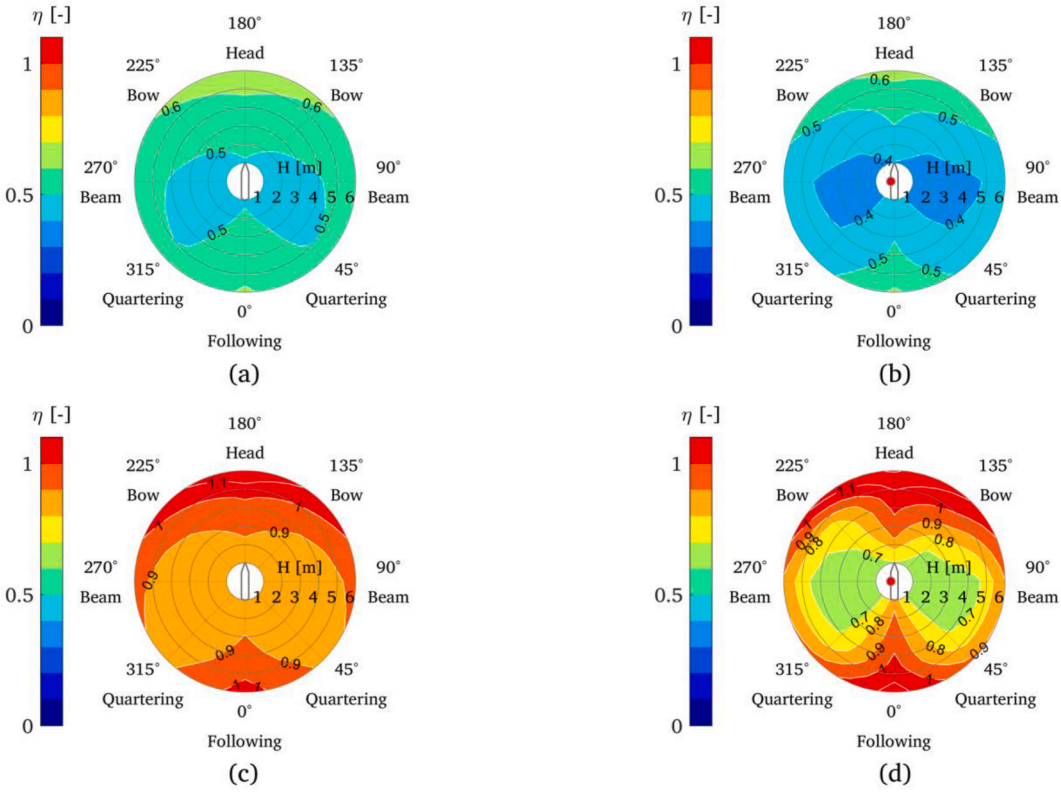

Fig. 21. Structural adequacy polar diagrams for four structural conditions: **(a)** T-1-I, **(b)** T-1-D, **(c)** T-5-I and **(d)** T-5-D. Red dot indicates collision damage location. (For interpretation of the references to colour in this figure legend, the reader is referred to the Web version of this article.)

3.4. Discussion

Motion and force analyses reaffirmed that an intact ship in head or following waves is subject to pure vertical bending loads. The weight distribution of the case study tanker with empty tanks resulted in hogging still water bending moments. Nevertheless, this condition is violated for all other wave-encountering directions. Moreover, for a damaged ship, biaxial bending will arise even at wave-encountering directions of 0° and 180° due to roll motions induced by the ship list. Today's practices require that the residual strength of a damaged vessel be compared against the prescribed vertical bending moment, with safety factors applied to account for rotation of the bending neutral axis due to asymmetry of the damaged cross-section under load. Given that neutral axis rotation may be caused by both cross-section and loading asymmetry, one may presume that the currently effective guidelines and rules may overlook the realistic loading conditions arising after an impact-related accident.

In addition, the damaged stability simulations and force analyses revealed a decrease in the hogging moment for the tanker struck in a collision. The increase in weight across damaged compartments due to flooding amidships forced redistribution of the loads towards sagging conditions. From a structural safety perspective, the decrease in load for an as-built tanker is advantageous. However, the risk of progressive collapse was found to increase for the same but severely corroded tanker in some sea states. To mitigate that risk, a ship must be oriented to meet beam or quartering waves. This conclusion is contradictory from the ship stability perspective since beam waves may lead to excessive roll motions and increased risk of capsizing. While capsizing is not a major hazard for a tanker, it can be for vessels with a slender hull and a high center of gravity such as a RoPax or a containership [13]. Thus, to decrease the consequences of an accident, ship stability, structural safety and their interplay should all be considered when taking risk mitigation measures.

Furthermore, the presumed presence of cargo or ballast water will contribute to variability in the still water bending loads, including a shift to sagging conditions. Note that a single upper deck and double bottom structural arrangement of the tanker means lower ultimate strength in sagging compared to hogging. Thus, for a fully loaded tanker, a further reduction in strength together with an enhanced sagging moment associated with breach of the structural and watertight integrity may increase the risk of ULS attainment. To either support or disprove this hypothesis, the SHARC model should be further developed to include the interaction and mixing of fluids with different properties, such as sea water and oil, to establish a realistic weight and load distribution during flooding, e.g., see Refs. [37,38]. This development will also enable predictions of the fluid cargo outflow rate and volume necessary for the assessment of accident consequences for the environment.

Additionally, the longitudinal location of accidental damage may play a crucial role in structural safety due to the varying onset locations and amplitudes of acting loads during vessel motions in waves. The spread of the moment onset location depends to a large extent on the amplitude of pitch motions that are defined by the weight distribution and wave characteristics. Thus, a tolerable impact located aside from midships in most situations may pose the danger of progressive collapse in certain loading conditions. With prior knowledge about the actual dynamic bending load distribution, preventive countermeasures may be planned, and actions may be taken accordingly (if possible) to expose the less loaded sections when impact is unavoidable.

A vast number of disclosed parameters influencing ship safety elicit the expedience of a limit state design, which is based on explicit consideration of the various conditions under which the structure may fail to fulfill its designated functions [14]. The presented safety assessment methodology has proved its potential to be an effective tool for ship design according to the limit state principles. With predefined models, ship stability simulations in SIMCAP and structural safety assessments in URSA, i.e., the two modules of SHARC, can be accomplished within several minutes. Thus, an admissible accurate and rapid check for ship design compliance with the required safety level is enabled.

The final discussed application of the proposed SHARC methodology is an example of how the passive safety of a ship may be enhanced through application of the ultimate and accidental limit state principles during design to obtain a stable, sufficiently strong and crashworthy hull. Furthermore, passive safety may be complemented by active safety measures such as collision avoidance, the minimization of accident consequences by the maneuvering and positioning of a vessel, and counterflooding. Models based on simplified methods that provide the ability for analyses in real time with acceptable fidelity, such as SHARC, may be used as decision support for masters and acting authorities or directly implemented in ship automated systems. The implementation of active safety is supported by ongoing digitalization of the shipping industry and emerging trends in autonomous solutions.

4. Conclusions

This study revealed that to ensure an adequate level of safety in damaged conditions, realistic estimations of the hull girder responses and strength are required. Therefore, a new methodology for ship safety assessment under transient conditions was proposed, where ultimate strength analyses are coupled with time-domain-based ship motion simulations with progressive flooding. In addition, a new methodology for structural safety assessments was presented. The new method considers the longitudinally varying biaxial ultimate strength of an intact or damaged vessel subjected to time-variant loads.

An investigation of the motions and loads of a damaged vessel revealed excessive roll and the constant presence of biaxial bending at all sea states. No risk of capsizing was reported for a tanker with watertight integrity breach of a single cargo hold amidships. Although a reduction in the hogging moment due to flooding of a tanker with initially empty tanks was observed, structural safety may be compromised when certain conditions are met. Moreover, not only the collision damage extent and its vertical location but also the longitudinal position of the impact along the struck ship determines its postaccident structural safety.

The SHARC methodology facilitates investigation of how different parameters and their interactions will affect both the stability and structural safety of a vessel. The parameters that can be studied are, among others, the structural arrangement and hull form of a

vessel, deterioration due to corrosion, accidental impact, different cargo loading conditions and weather conditions. The influence of these parameters can be studied in terms of the motion and load amplitudes, time to flooding or eventual capsize and structural adequacy measures. The output from the developed model provides firm ground for further risk analyses with respect to stability, accidents or environmental damage.

Declaration of competing interest

The authors declare that there is no known competing financial interests or personal relationships that could have influenced the work presented in the paper.

Acknowledgements

This study received financial support from the Swedish Transport Administration project "SHARC - Structural and Hydro mechanical Assessment of Risk in Collision and grounding" (grant agreement: TRV 2019/42277). The FEAs were partly performed on resources at the Chalmers Centre for Computational Science and Engineering (C3SE www.c3se.chalmers.se) provided by the Swedish National Infrastructure for Computing (SNIC).

References

[1] Paik JK. Advanced structural safety studies. first ed., vol. 37. Singapore: Springer Nature Singapore Pte Ltd.; 2020. https://doi.org/10.1007/978-981-13-8245-1.
[2] Santos TA, Guedes Soares C. Numerical assessment of factors affecting the survivabili'ty of damaged ro-ro ships in waves. Ocean Eng 2009;36:797–809. https://doi.org/10.1016/j.oceaneng.2009.04.004.
[3] Bennett SS, Phillips AB. Experimental investigation of the influence of floodwater due to ship grounding on motions and global loads. Ocean Eng 2017;130:49–63. https://doi.org/10.1016/j.oceaneng.2016.11.039.
[4] Ruponen P, Lindroth D, Routi AL, Aartovaara M. Simulation-based analysis method for damage survivability of passenger ships. Ship Technol Res 2019;66:180–92. https://doi.org/10.1080/09377255.2019.1598629.
[5] Manderbacka T, Themelis N, Bačkalov I, Boulougouris E, Eliopoulou E, Hashimoto H, et al. An overview of the current research on stability of ships and ocean vehicles: the STAB2018 perspective. Ocean Eng 2019;186. https://doi.org/10.1016/j.oceaneng.2019.05.072.
[6] Zhang XL, Lin Z, Li P, Liu DK, Li Z, Pang ZW, et al. A numerical investigation on the effect of symmetric and asymmetric flooding on the damage stability of a ship. J Mar Sci Technol 2020;25:1151–65. https://doi.org/10.1007/s00773-020-00706-9.
[7] Campanile A, Piscopo V, Scamardella A. Time-variant bulk carrier reliability analysis in pure bending intact and damage conditions. Mar Struct 2016;46:193–228. https://doi.org/10.1016/j.marstruc.2016.02.003.
[8] Parunov J, Prebeg P, Rudan S. Post-accidental structural reliability of double-hull oil tanker with near realistic collision damage shapes. Ships Offshore Struct 2020:1–18. https://doi.org/10.1080/17445302.2020.1789035.
[9] Revised IMO. Interim guidelines for the approval of alternative methods of design and con- struction of oil tankers under regulation 13F(5) of annex I of MARPOL 3/78. Resolution MEPC 2003;110(49). Annex 16. 2003.
[10] IMO. Goal-based new ship construction standards: linkage between FSA and GBS MSC 81/INF.6. 2006.
[11] Kuznecovs A, Ringsberg JW, Johnson E, Yamada Y. Ultimate limit state analysis of a double-hull tanker subjected to biaxial bending in intact and collision-damaged conditions. Ocean Eng 2020;209. https://doi.org/10.1016/j.oceaneng.2020.107519.
[12] Hogström P, Ringsberg JW. An extensive study of a ship's survivability after collision - a parameter study of material characteristics, non-linear FEA and damage stability analyses. Mar Struct 2012;27:1–28. https://doi.org/10.1016/j.marstruc.2012.03.001.
[13] Schreuder M, Hogström P, Ringsberg JW, Johnson E, Janson CE. A method for assessment of the survival time of a ship damaged by collision. Trans - Soc Nav Archit Mar Eng 2011;119:603–19.
[14] Paik JK. Ultimate limit state analysis and design of plated structures. second ed. Hoboken, NJ: John Wiley & Sons; 2018. https://doi.org/10.1002/9781119367758.
[15] Ringsberg JW, Li Z, Johnson E, Kuznecovs A, Shafieisabet R. Reduction in ultimate strength capacity of corroded ships involved in collision accidents. Ships Offshore Struct 2018;13:155–66. https://doi.org/10.1080/17445302.2018.1429158.
[16] Schreuder M. Development, implementation, validation and applications of a method for simulation of damaged and intact ships in waves. Chalmers University of Technology; 2014.
[17] Kuznecovs A. Ultimate and residual strength assessment of ship structures. Chalmers University of Technology; 2020.
[18] Rawson C, Crake K, Brown AJ. Assessing the environmental performance of tankers in accidental groundings and collisions. Trans - Soc Nav Archit Mar Eng 1998;106:41–58.
[19] Lützen M. Ship collision damage. Technical University of Denmark; 2001.
[20] Brown AJ. Collision scenarios and probabilistic collision damage. Mar Struct 2002;15:335–64. https://doi.org/10.1016/S0951-8339(02)00007-2.
[21] Ringsberg JW, Li Z, Johnson E. Performance assessment of the crashworthiness of corroded ship hulls. In: Prog. Anal. Des. Mar. Struct. - proc. 6th int. Conf. Mar. Struct. MARSTRUCT 2017; 2017. p. 523–31. https://doi.org/10.1201/9781315157368-60. Lisbon, Portugal.
[22] Baxevanis D. Residual strength assessment of corroded ships involved in ship-to-ship collisions. Chalmers University of Technology; 2019.
[23] Common IACS. Structural rules for bulk carriers and oil tankers. 2019.
[24] Garbatov Y, Parunov J, Kodvanj J, Saad-Eldeen S, Guedes Soares C. Experimental assessment of tensile strength of corroded steel specimens subjected to sandblast and sandpaper cleaning. Mar Struct 2016;49:18–30.
[25] Dassault Systèmes Simulia Corp. Abaqus analysis user's guide. 2013.
[26] Cummins WE. The impulse response function and ship motions. In: Symp. Sh. Theory, institut für schiffbau der universität hamburg:; 1962.
[27] Faltinsen OM. Sea loads on ships and offshore structures. Cambridge, UK: Cambridge University Press; 1990.
[28] Spanos DA, Papanikolaou AD. Comparative study of numerical simulation methods on the prediction of parametric roll of ships in waves. Mar Technol Eng 2011;1:653–60.
[29] Smith CS. Influence of local compressive failure on ultimate longitudinal strength of a ship's hull. PRADS - Int Symp Pract Des Shipbuild 1977:73–9.
[30] Dnv GL. Rules for classification, ships, Part 3 hull. 2019 [Chapter 5] Hull girder strength.
[31] Rules BV. For the classification of steel ships, Part B - hull and stability, NR 467. Bureau Veritas Marine & Offshore; 2020. B1. Paris, France.
[32] Fujikubo M, Takemura K, Oka S, Alie MZM, Iijima K. Residual hull girder strength of asymmetrically damaged ships. J Japan Soc Nav Archit Ocean Eng 2012;16:131–40.
[33] Gordo JM, Guedes Soares C. Interaction equation for the collapse of tankers and containerships under combined bending moments. J Ship Res 1997;41:230–40.
[34] Maib M. Report on the investigation of the structural failure of MSC Napoli English channel on 18 january 2007. 2008. Southampton, United Kingdom.
[35] Dang Van K, Cailletaud G, Flavenot JF, Le Douaron A, Lieurade HP. Criterion for high cycle fatigue failure under multuiaxial loading. In: Brown MW, Miller KJ, editors. Int. Conf. Biaxial/multiaxial fatigue (2nd 1985 univ. Sheffield). London: Mechanical Engineering Publications; 1989. p. 479–96.

[36] Standards Norway. NORSOK: N-004: design of steel structures. Nor Oil Ind Assoc Fed Nor Manuf Ind 2004;N-004.
[37] Tavakoli MT, Amdahl J, Leira BJ. Analytical and numerical modelling of oil spill from a side tank with collision damage. Ships Offshore Struct 2012;7:73–86. https://doi.org/10.1080/17445302.2010.537844.
[38] Kollo M, Laanearu J. Hydraulic modelling of oil spill through submerged orifices in damaged ship hulls. Ocean Eng 2017;130:385–97. https://doi.org/10.1016/j.oceaneng.2016.11.032.